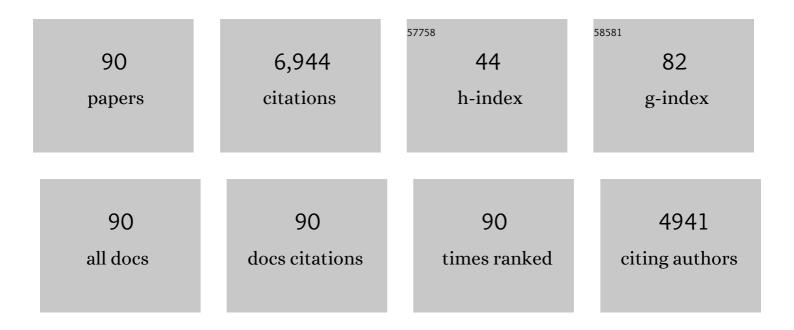
List of Publications by Year in descending order

Source: https://exaly.com/author-pdf/592175/publications.pdf Version: 2024-02-01



#	Article	IF	CITATIONS
1	Compared effects of "solid-based―hydrogen peroxide pretreatment on disintegration and properties of waste activated sludge. Chinese Chemical Letters, 2022, 33, 1293-1297.	9.0	16
2	Insights into removal of sulfonamides in anaerobic activated sludge system: Mechanisms, degradation pathways and stress responses. Journal of Hazardous Materials, 2022, 423, 127248.	12.4	30
3	Effect of substrate structure on medium chain fatty acids production and reactor microbiome. Environmental Research, 2022, 204, 111947.	7.5	21
4	Peroxydisulfate bridged photocatalysis of covalent triazine framework for carbamazepine degradation. Chemical Engineering Journal, 2022, 427, 131613.	12.7	18
5	Enhanced utilization efficiency of peroxymonosulfate via water vortex-driven piezo-activation for removing organic contaminants from water. Environmental Science and Ecotechnology, 2022, 10, 100165.	13.5	49
6	Mutual interaction between the secreted flavins and immobilized quinone in anaerobic removal of high-polarity aromatic compounds containing nitrogen by Shewanella sp. RQs-106. Journal of Hazardous Materials, 2022, 431, 128595.	12.4	5
7	Simultaneous medium chain fatty acids production and process carbon emissions reduction in a continuous-flow reactor: Re-understanding of carbon flow distribution. Environmental Research, 2022, 212, 113294.	7.5	5
8	Spin-states-assistance peroxymonosulfate absorption via Mn doped catalyst with/without light for BPA oxidation: The negative contribution of electrons transfer by light. Chemical Engineering Journal, 2022, 443, 136399.	12.7	18
9	Atomically dispersed cobalt on carbon nitride for peroxymonosulfate activation: Switchable catalysis enabled by light irradiation. Chemical Engineering Journal, 2022, 446, 137277.	12.7	19
10	Developing functional carbon nitride materials for efficient peroxymonosulfate activation: From interface catalysis to irradiation synergy. , 2022, 1, 21-33.		1
11	Dissecting the roles of conductive materials in attenuating antibiotic resistance genes: Evolution of physiological features and bacterial community. Journal of Hazardous Materials, 2022, 438, 129411.	12.4	5
12	Structure–dependent degradation of nitroimidazoles by cobalt–manganese layered double hydroxide catalyzed peroxymonosulfate process. Chemosphere, 2021, 266, 129006.	8.2	34
13	Alkylethoxyglucoside-enhanced volatile fatty acids production from waste activated sludge: Performance and mechanisms. Journal of Cleaner Production, 2021, 289, 125765.	9.3	20
14	Insight into the effects of hydroxyl groups on the rates and pathways of tetracycline antibiotics degradation in the carbon black activated peroxydisulfate oxidation process. Journal of Hazardous Materials, 2021, 412, 125256.	12.4	70
15	Insights into the oxidation of organic contaminants by Co(II) activated peracetic acid: The overlooked role of high-valent cobalt-oxo species. Water Research, 2021, 201, 117313.	11.3	106
16	Non-covalent doping of carbon nitride with biochar: Boosted peroxymonosulfate activation performance and unexpected singlet oxygen evolution mechanism. Chemical Engineering Journal, 2021, 418, 129504.	12.7	64
17	Novel Nonradical Oxidation of Sulfonamide Antibiotics with Co(II)-Doped g-C ₃ N ₄ -Activated Peracetic Acid: Role of High-Valent Cobalt–Oxo Species. Environmental Science & Technology, 2021, 55, 12640-12651.	10.0	115
18	Peroxymonosulfate activation by cobalt(II) for degradation of organic contaminants via high-valent cobalt-oxo and radical species. Journal of Hazardous Materials, 2021, 416, 125679.	12.4	27

#	Article	IF	CITATIONS
19	Multipath elimination of bisphenol A over bifunctional polymeric carbon nitride/biochar hybrids in the presence of persulfate and visible light. Journal of Hazardous Materials, 2021, 417, 126008.	12.4	35
20	Deciphering the transfers of antibiotic resistance genes under antibiotic exposure conditions: Driven by functional modules and bacterial community. Water Research, 2021, 205, 117672.	11.3	76
21	Bio-CQDs surface modification BiOCl for the BPA elimination and evaluation in visible light: The contribution of C-localized level. Journal of Colloid and Interface Science, 2021, 602, 1-13.	9.4	28
22	Consolidated 3D Co3Mn-layered double hydroxide aerogel for photo-assisted peroxymonosulfate activation in metronidazole degradation. Chemical Engineering Journal, 2021, 423, 130172.	12.7	48
23	Opportunities and challenges in microbial medium chain fatty acids production from waste biomass. Bioresource Technology, 2021, 340, 125633.	9.6	48
24	Difunctional carbon quantum dots/g-C3N4 with in-plane electron buffer for intense tetracycline degradation under visible light: Tight adsorption and smooth electron transfer. Applied Catalysis B: Environmental, 2021, 299, 120694.	20.2	84
25	Inhibition of biofouling in membrane bioreactor by metabolic uncoupler based on controlling microorganisms accumulation and quorum sensing signals secretion. Chemosphere, 2020, 245, 125363.	8.2	12
26	New insight into the substituents affecting the peroxydisulfate nonradical oxidation of sulfonamides in water. Water Research, 2020, 171, 115374.	11.3	88
27	Sludge-derived biochar as efficient persulfate activators: Sulfurization-induced electronic structure modulation and disparate nonradical mechanisms. Applied Catalysis B: Environmental, 2020, 279, 119361.	20.2	240
28	In situ photoreduction of structural Fe(III) in a metal–organic framework for peroxydisulfate activation and efficient removal of antibiotics in real wastewater. Journal of Hazardous Materials, 2020, 388, 121996.	12.4	121
29	Long-term medium chain carboxylic acids production from liquor-making wastewater: Parameters optimization and toxicity mitigation. Chemical Engineering Journal, 2020, 388, 124218.	12.7	59
30	Enhanced removal of sulfadiazine by sulfidated ZVI activated persulfate process: Performance, mechanisms and degradation pathways. Chemical Engineering Journal, 2020, 388, 124303.	12.7	112
31	B-doped graphitic porous biochar with enhanced surface affinity and electron transfer for efficient peroxydisulfate activation. Chemical Engineering Journal, 2020, 396, 125119.	12.7	148
32	Activation of peroxymonosulfate by cobalt-impregnated biochar for atrazine degradation: The pivotal roles of persistent free radicals and ecotoxicity assessment. Journal of Hazardous Materials, 2020, 398, 122768.	12.4	100
33	Carbon quantum dots-based semiconductor preparation methods, applications and mechanisms in environmental contamination. Chinese Chemical Letters, 2020, 31, 2556-2566.	9.0	49
34	Concentrating lactate-carbon flow on medium chain carboxylic acids production by hydrogen supply. Bioresource Technology, 2019, 291, 121573.	9.6	46
35	Edge-nitrogenated biochar for efficient peroxydisulfate activation: An electron transfer mechanism. Water Research, 2019, 160, 405-414.	11.3	566
36	Medium chain carboxylic acids production from waste biomass: Current advances and perspectives. Biotechnology Advances, 2019, 37, 599-615.	11.7	187

#	Article	IF	CITATIONS
37	Degradation pathways and kinetics of anthraquinone compounds along with nitrate removal by a newly isolated Rhodococcus pyridinivorans GF3 under aerobic conditions. Bioresource Technology, 2019, 285, 121336.	9.6	18
38	Biochar-induced Fe(III) reduction for persulfate activation in sulfamethoxazole degradation: Insight into the electron transfer, radical oxidation and degradation pathways. Chemical Engineering Journal, 2019, 362, 561-569.	12.7	220
39	Singlet oxygen-dominated peroxydisulfate activation by sludge-derived biochar for sulfamethoxazole degradation through a nonradical oxidation pathway: Performance and mechanism. Chemical Engineering Journal, 2019, 357, 589-599.	12.7	363
40	Hydroxyl radical dominated degradation of aquatic sulfamethoxazole by Fe0/bisulfite/O2: Kinetics, mechanisms, and pathways. Water Research, 2018, 138, 323-332.	11.3	236
41	Electro-peroxone pretreatment for enhanced simulated hospital wastewater treatment and antibiotic resistance genes reduction. Environment International, 2018, 115, 70-78.	10.0	64
42	Enhanced peroxymonosulfate activation for sulfamethazine degradation by ultrasound irradiation: Performances and mechanisms. Chemical Engineering Journal, 2018, 335, 145-153.	12.7	269
43	Selective degradation of sulfonamide antibiotics by peroxymonosulfate alone: Direct oxidation and nonradical mechanisms. Chemical Engineering Journal, 2018, 334, 2539-2546.	12.7	284
44	Weak magnetic field for enhanced oxidation of sulfamethoxazole by Fe0/H2O2 and Fe0/persulfate: Performance, mechanisms, and degradation pathways. Chemical Engineering Journal, 2018, 351, 532-539.	12.7	55
45	Effect of metabolic uncoupler, 3,3′,4′,5-tetrachlorosalicylanilide (TCS) on <i>Bacillus subtilis</i> : biofilm formation, flocculability and surface characteristics. RSC Advances, 2018, 8, 16178-16186.	3.6	7
46	Inhibition of biofilm formation by chemical uncoupler, 3, 3′, 4′, 5-tetrachlorosalicylanilide (TCS): From the perspective of quorum sensing and biofilm related genes. Biochemical Engineering Journal, 2018, 137, 95-99.	3.6	10
47	Upgrading liquor-making wastewater into medium chain fatty acid: Insights into co-electron donors, key microflora, and energy harvest. Water Research, 2018, 145, 650-659.	11.3	147
48	Simultaneous bisphenol F degradation, heterotrophic nitrification and aerobic denitrification by a bacterial consortium. Journal of Chemical Technology and Biotechnology, 2017, 92, 854-860.	3.2	22
49	Heteroatoms doped graphene for catalytic ozonation of sulfamethoxazole by metal-free catalysis: Performances and mechanisms. Chemical Engineering Journal, 2017, 317, 632-639.	12.7	107
50	Factors affecting p-nitrophenol removal by microscale zero-valent iron coupling with weak magnetic field (WMF). RSC Advances, 2017, 7, 18231-18237.	3.6	23
51	Adsorption of p-nitrophenols (PNP) on microalgal biochar: Analysis of high adsorption capacity and mechanism. Bioresource Technology, 2017, 244, 1456-1464.	9.6	144
52	Enhancing sludge biodegradability and volatile fatty acid production by tetrakis hydroxymethyl phosphonium sulfate pretreatment. Bioresource Technology, 2017, 239, 518-522.	9.6	32
53	Degradation of sulfamethoxazole by a heterogeneous Fenton-like system with microscale zero-valent iron: Kinetics, effect factors, and pathways. Journal of the Taiwan Institute of Chemical Engineers, 2017, 81, 232-238.	5.3	43
54	Enhanced volatile fatty acid production from excess sludge by combined free nitrous acid and rhamnolipid treatment. Bioresource Technology, 2017, 224, 727-732.	9.6	46

#	Article	IF	CITATIONS
55	Mathematical modeling of simultaneous carbon-nitrogen-sulfur removal from industrial wastewater. Journal of Hazardous Materials, 2017, 321, 371-381.	12.4	17
56	Surfactant (CTAB) assisted flower-like Bi2WO6 through hydrothermal method: Unintentional bromide ion doping and photocatalytic activity. Catalysis Communications, 2017, 88, 68-72.	3.3	49
57	Removal of cephalosporin antibiotics 7-ACA from wastewater during the cultivation of lipid-accumulating microalgae. Bioresource Technology, 2016, 221, 284-290.	9.6	125
58	Degradation of sulfadiazine in water by a UV/O ₃ process: performance and degradation pathway. RSC Advances, 2016, 6, 57138-57143.	3.6	39
59	Enhancement of volatile fatty acid production by co-fermentation of food waste and excess sludge without pH control: The mechanism and microbial community analyses. Bioresource Technology, 2016, 216, 653-660.	9.6	175
60	Enhanced sulfamethoxazole ozonation by noble metal-free catalysis based on magnetic Fe ₃ O ₄ nanoparticles: catalytic performance and degradation mechanism. RSC Advances, 2016, 6, 19265-19270.	3.6	40
61	Promotion effects of ultrasound on sludge biodegradation by thermophilic bacteria Geobacillus stearothermophilus TP-12. Biochemical Engineering Journal, 2016, 105, 281-287.	3.6	9
62	Economical evaluation of sludge reduction and characterization of effluent organic matter in an alternating aeration activated sludge system combining ozone/ultrasound pretreatment. Bioresource Technology, 2015, 177, 194-203.	9.6	33
63	Enhanced amoxicillin treatment using the electro-peroxone process: key factors and degradation mechanism. RSC Advances, 2015, 5, 52695-52702.	3.6	50
64	Enhancement of volatile fatty acid production using semi-continuous anaerobic food waste fermentation without pH control. RSC Advances, 2015, 5, 103876-103883.	3.6	17
65	Sulfamethoxazole degradation by ultrasound/ozone oxidation process in water: Kinetics, mechanisms, and pathways. Ultrasonics Sonochemistry, 2015, 22, 182-187.	8.2	145
66	Reduction of 4-chloronitrobenzene in a bioelectrochemical reactor with biocathode at ambient temperature for a long-term operation. Journal of the Taiwan Institute of Chemical Engineers, 2015, 46, 119-124.	5.3	16
67	Optimization of ultrasonic pretreatment and substrate/inoculum ratio to enhance hydrolysis and volatile fatty acid production from food waste. RSC Advances, 2014, 4, 53321-53326.	3.6	31
68	Thermophilic hydrogen production from sludge pretreated by thermophilic bacteria: Analysis of the advantages of microbial community and metabolism. Bioresource Technology, 2014, 172, 433-437.	9.6	43
69	Simultaneous nutrient removal and reduction in sludge from sewage waste using an alternating anaerobic–anoxic–microaerobic–aerobic system combining ozone/ultrasound technology. RSC Advances, 2014, 4, 52892-52897.	3.6	17
70	Possible causes of excess sludge reduction adding metabolic uncoupler, 3,3′,4′,5-tetrachlorosalicylanilide (TCS), in sequence batch reactors. Bioresource Technology, 2014, 173, 96-103.	9.6	51
71	Accelerated startup of hydrogen production expanded granular sludge bed with l-Cysteine supplementation. Energy, 2013, 60, 94-98.	8.8	24
72	Treatability study of 3,3′,4′,5-tetrachlorosalicylanilide (TCS) combined with 2,4,6-trichlorophenol (TCP) to reduce excess sludge production in a sequence batch reactor. Bioresource Technology, 2013, 143, 642-646.	9.6	16

#	Article	IF	CITATIONS
73	Ultrasonic-assisted ozone oxidation process of triphenylmethane dye degradation: Evidence for the promotion effects of ultrasonic on malachite green decolorization and degradation mechanism. Bioresource Technology, 2013, 128, 827-830.	9.6	66
74	Minimization of excess sludge production by in-situ activated sludge treatment processes — A comprehensive review. Biotechnology Advances, 2013, 31, 1386-1396.	11.7	180
75	Characterizing the fluorescent products of waste activated sludge in dissolved organic matter following ultrasound assisted ozone pretreatments. Bioresource Technology, 2013, 131, 560-563.	9.6	56
76	Application of low frequency ultrasound to stimulate the bio-activity of activated sludge for use as an inoculum in enhanced hydrogen production. RSC Advances, 2013, 3, 21848.	3.6	20
77	Photo-hydrogen production by Rhodopseudomonas faecalis RLD-53 immobilized on the surface of modified activated carbon fibers. RSC Advances, 2012, 2, 2225.	3.6	21
78	Continuous photo-hydrogen production in anaerobic fluidized bed photo-reactor with activated carbon fiber as carrier. RSC Advances, 2012, 2, 5531.	3.6	18
79	Simultaneous waste activated sludge disintegration and biological hydrogen production using an ozone/ultrasound pretreatment. Bioresource Technology, 2012, 124, 347-354.	9.6	94
80	A rapid and low energy consumption method to decolorize the high concentration triphenylmethane dye wastewater: Operational parameters optimization for the ultrasonic-assisted ozone oxidation process. Bioresource Technology, 2012, 105, 40-47.	9.6	33
81	Treatability study of using low frequency ultrasonic pretreatment to augment continuous biohydrogen production. International Journal of Hydrogen Energy, 2011, 36, 14180-14185.	7.1	31
82	Optimization of operating parameters for sludge process reduction under alternating aerobic/oxygen-limited conditions by response surface methodology. Bioresource Technology, 2011, 102, 9843-9851.	9.6	55
83	Biological hydrogen production by dark fermentation: challenges and prospects towards scaled-up production. Current Opinion in Biotechnology, 2011, 22, 365-370.	6.6	180
84	Optimization of key variables for the enhanced production of hydrogen by Ethanoligenens harbinense W1 using response surface methodology. International Journal of Hydrogen Energy, 2011, 36, 5843-5848.	7.1	25
85	Accelerated startup of biological hydrogen production process by addition of Ethanoligenens harbinense B49 in a biofilm-based column reactor. International Journal of Hydrogen Energy, 2010, 35, 13407-13412.	7.1	18
86	Biological hydrogen production from organic wastewater by dark fermentation in China: Overview and prospects. Frontiers of Environmental Science and Engineering in China, 2009, 3, 375-379.	0.8	16
87	Optimization of culture conditions for hydrogen production by Ethanoligenens harbinense B49 using response surface methodology. Bioresource Technology, 2009, 100, 1192-1196.	9.6	147
88	Biohydrogen production from ethanol-type fermentation of molasses in an expanded granular sludge bed (EGSB) reactor. International Journal of Hydrogen Energy, 2008, 33, 4981-4988.	7.1	143
89	Dark fermentation of xylose and glucose mix using isolated Thermoanaerobacterium thermosaccharolyticum W16. International Journal of Hydrogen Energy, 2008, 33, 6124-6132.	7.1	180
90	Ultrasonic-assisted ozone oxidation process for sulfamethoxazole removal: impact factors and degradation process. Desalination and Water Treatment, 0, , 1-8.	1.0	4